



**New trends from young scientists
in Molecular
and Atomic Physics**

JD 5000
83-0200
AT. NO.
MILWAUKEE

Edited by:

Antonio Sánchez Coronilla, José María Carnerero Panduro, Inmaculada Márquez Escudero, José Antonio Lebrón Romero, Aila Jiménez Ruiz, Francisco José Ostos Marcos, Elena Rodríguez Remesal, Eva Pérez Bernal.

Published by:

Secretariado de Recursos Audiovisuales y Nuevas Tecnologías, Universidad de Sevilla

Published in:

March 2017

ISBN:

978-84-16784-65-3



**New trends from young scientists in
Molecular and Atomic Physics**

INDEX

Foreword and introduction	1
Biophysic and Biomolecules	2
➤ Collagen and Chitosan-based Membranes Processed by Electrospinning for Tissue Engineering	3
➤ Study of the Influence of MMT Nanoparticles Concentration in Soy-based Bioplastics Obtained by Injection Moulding	9
➤ Scaffolds Produced Using Biopolymer Matrices (Collagen/Chitosan) with Application in Tissue Engineering	15
➤ Development of Superabsorbent Biodegradable Materials Derived from Soy Protein Isolate	20
➤ Relationship between Emulsion Stability and Interfacial Properties of Legume-based Systems (“ <i>Vicia Faba</i> ”)	26
➤ Development of Superabsorbent Matrix in Horticulture through Incorporation of Micronutrients	32
➤ Radiobiology for Improving Boron Neutron Capture Therapy Treatment Planning	38
Nanoparticles and Aggregates	43
➤ Influence of pH in the Interaction Adenine-Gold Nanoparticles	44
➤ Effect of Citrate Stabilization over Gold Nanoparticle Systems	50
➤ Propagation of 3D Wave Packets to Study the Sieving of Helium Isotopes through Carbon-based Nanoporous Membranes	55
➤ MoS ₂ /TiO ₂ Mixture: An Example of Modification Strategies of TiO ₂ Nanoparticles to Improve Photocatalytic Activity	63
➤ Experimental and Theoretical Research on Heat Transfer Characteristics of Ethylene Glycol-based Nanofluids Containing Nickel Nanoparticles	69
➤ Application of Ag-nanofluid for Concentrating Solar Power: Experimental Characterization and Molecular Dynamics Study	75
Spectroscopy, Chromatography, Calorimetry, Electrochemistry and X-Ray Applications	81

➤ Natural and Cheap Carbonates for Thermochemical Energy Storage of Concentrated Solar Power	82
➤ Ionic Surfactants Interactions with Carboxylated Single-Walled Carbon Nanotubes	88
➤ Atomic Plasma Physics In The Interaction of Ultra-Short and Ultra-Intense X-Ray Laser with Matter	94
➤ Kinetic Analysis of Crosslinking Processes of Polysilazane and Polysiloxane Polymeric Precursors by DSC	99
➤ Self-assembled Monolayers of Acidic Thiols: Dielectric Behavior	105
➤ Host-Guest Complexes between Surfactants and Cyclodextrins in Aqueous Solutions. Effects of the Inclusion of a Functional Group at the End of the Surfactant Tail	111
➤ Enhanced and Exotic Laser Performance in Novel BODIPY Dyes	120
➤ Approaches to the Study of Circumstellar Discs	126
Computational Modeling, Conformational Analysis and Reactivity of Chemical Systems	132
➤ Heisenberg-Like Uncertainty Measures for D-Dimensional Hydrogenic Systems at Large D	133
➤ Generalized Quantum Similarity in Atomic Systems: A Quantifier of Relativistic Effects	139
➤ Temporal Evolution of the Hydrogen Atom after Confinement	144
➤ Noncovalent Interactions between Cisplatin and Graphene Prototypes	150
➤ Femtosecond Photodissociation Dynamics of Chloriodomethane in the First Absorption Band	157
➤ Quantum Properties of a Binary Bosonic Mixture in a Double Well	163
➤ An Experimental and Theoretical Study for a Cu-H ₂ O Nanofluid	169
➤ Effects of Microsolvation in the Lactim-Lactam Tautomerism of 2-Hydroxypyridine/2-Pyridone	175
➤ Using Surfactant as Stabilizers of NiO Nanofluids: An Experimental and Theoretical Viewpoint	182
➤ On the Tetragonal Perovskite CH ₃ NH ₃ PbI ₃ . Analysis of the Substitution of A and B Sites	188

➤ Molecular Dynamics Simulations of Metal-Nanofluid. Modelling their Thermophysical Properties for Using on Concentrating Solar Power Plants	194
➤ Structural, Electronic and Optical Properties of Room-Temperature-Stable Polymorphs of Copper, Silver and Gold Sulfides: A Density Functional Study	202
➤ Potassium Single Atom Adsorption on TiO ₂ (110) Surface and the Role of Water	207
➤ Theoretical Insights on Astrochemical Reactions Catalyzed by Interstellar Dust Grain Surfaces	214
➤ Imaging the Photodissociation Dynamics of the Methyl Radical from the 3s and 3pz Rydberg States	218
Main author index	225

Noncovalent Interactions between Cisplatin and Graphene Prototypes

M. Refugio Cuevas, Massimiliano Bartolomei and Marco A. García-Revilla

1. Introduction

Cisplatin (CP) belongs to the most widely used anticancer drugs; it is the basis of a family of derivatives displaying a large anticancer activity, for example carboplatin and oxaliplatin. Nevertheless, CP displays a low bioavailability and for this reason the design of effective ways to reach the biological target is paramount and also very challenging¹. In recent years, the use of nanomaterials as drug delivery systems has become important^{2,3} and among them graphene (G), a two-dimensional material formed by a single layer of repeated hexagonal lattice of six atoms of carbon⁴, represents an ideal adsorbing platform. The physicochemical properties of G are related to its π -electrons conjugated system, which confers the capability of adsorbing different substances such as anti-cancer drugs, antibodies, peptides, DNA, RNA, genes⁵⁻⁸, etc. Recent reports have discussed the favourable physisorption of CP on carbon nanomaterials, like carbon nanotubes⁹ and nanohorns¹⁰. Also, the study of the non-covalent interactions of G and Graphene Oxides with adsorbed molecules holding a π -character, has been recently addressed¹¹.

In the present contribution Pyrene (P) was selected as the minimum prototype of G and its non-covalent interaction with CP was characterized by using a variety of electronic structure methodologies.

2. Results

The Coupled Second-order Moller-Plesset Perturbation Theory (MP2C)¹² was used as the reference method to obtain benchmark values of the interaction energies: the

used basis sets were the aug-cc-pVTZ-PP¹³ for Pt and the aug-cc-pVTZ¹⁴ for the rest of atoms. MP2C results were compared with standard MP2 interaction energies as well as with DFT estimations. For the latter the PBE¹⁵, B3LYP¹⁶ and M062X¹⁷ functionals were exploited together with the basis set 6-311+(2d,2p)¹⁸ for all atoms except Pt, for which the Stuttgart-Dresden pseudopotential¹⁹ was used. In the case of the PBE and B3LYP functionals, the latest dispersion correction ((D3)-BJ)²² contribution of Grimme, which includes the “damped dispersion” approach of Johnson-Becke (BJ)²³, was also taken into account. For all cases, rigid configurations of both monomers were used for the calculation of the interaction corresponding to their relative approach. All computed interaction energies were corrected for the Basis Set Superposition Error (BSSE)²⁰ by using the Counterpoise method²¹.

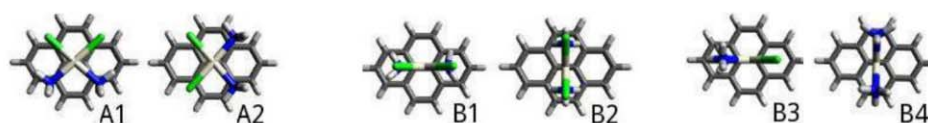


Figure 1. Main limiting configurations of the pyrene-cisplatin complex.

The six configurations of the P-CP complex that were selected are presented in Fig. 1. Moreover, the corresponding MP2C energy profiles are displayed in Fig. 2 as a function of the intermolecular distance joining the mass-centre of pyrene and the Pt atom and ranging from 8 to 2 Å. In the first panel of Fig. 2, almost equivalent energy profiles for the A1 and A2 configurations can be observed: the minimum of both configurations is located at about 3.5 Å, but A2 displays a slightly larger interaction energy of about 10.3 meV. In the second panel, the profiles of the B1 and B2 configurations are compared: the minimum of both configurations is found at larger distances and located around 4.75 Å; it can be also observed that the B1 well is deeper than that of B2 of about 38.4 meV. The results for the B3 and B4 perpendicular configurations are presented in the third and fourth panels, respectively: the minimum

of their energy profiles is located at even larger distances (around 5Å) being the corresponding wells quite shallower (-279.1 meV for B3 and -111.7 meV for B4) with respect to those for the other configurations.

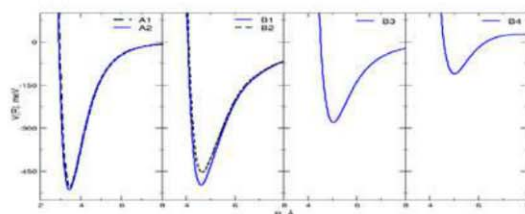


Figure 2. Interaction energies at the MP2C level for the A1, A2, B1 to B4 configurations of the pyrene-cisplatin complex.

Globally, the A2 (-511.73 meV) and B1 (-487.84) configurations are those showing the largest interaction energies, being A2 the more attractive profile. In order to make a simple comparison of methods, we have just selected the A2, B1, B3 and B4 configurations, and an analysis of the reliability of the related interaction energies at the MP2 and DFT and levels was performed, Figs. 3 and 4.

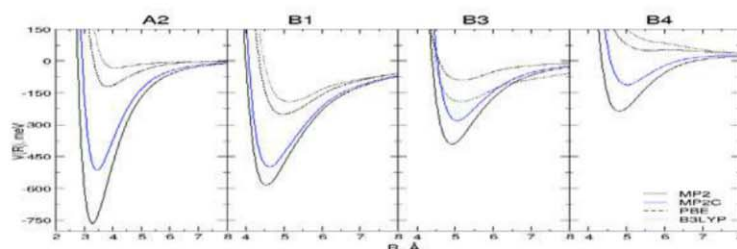


Figure 3. Interaction energies for the A2, B1, B3 and B4 configurations at the MP2C, MP2 and DFT levels.

In Fig. 3 the B3LYP and PBE results underestimate the reference MP2C interaction energies for all considered configurations, while MP2 energy overestimates such energy. The underestimation provided by the DFT results can be explained by considering that in general DFT fail to properly describe systems where the London

dispersion contribution to the interaction energy is relevant. To correct this deficiency, we also include the (D3)-BJ dispersion contribution to the PBE and B3LYP results. Such results are reported in Fig. 4 together with those carried out with the M062X functional, which indeed is in general a good option to describe van der Waals systems. It is clearly shown that the inclusion of the dispersion correction lead to a better agreement with the reference MP2C profiles. The B3LYP (D3)-BJ approach now provides an overestimation of the reference profiles, being such overestimation more significant for the A2 configuration. The M062X results are in general closer to the MP2C references in the well region; however, it must be noticed that the agreement get worse in the dissociation limit, where the M062X interaction energies draws away from the MP2C curve, especially for the perpendicular configurations.

The PBE (D3)-BJ results are indeed those providing the best agreement with the MP2C reference in the whole range of intermolecular distances for all selected configurations, being the energy difference around the minimum of 2.0%, 3.0%, 0.03% and 0.11% for A2, B1, B3 and B4, respectively. On top of that, the PBE (D3)-BJ approach has the advantage of being the most affordable method, among those considered, from the computational cost point of view.

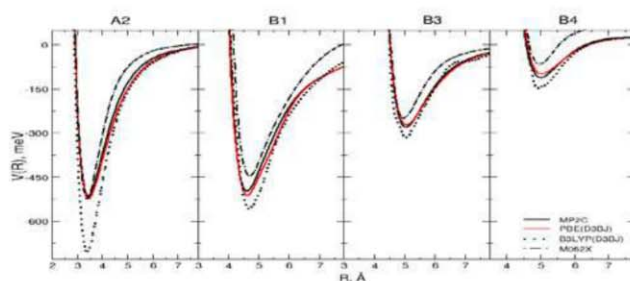


Figure 4. Interaction energies for the A2, B1, B3 and B4 configurations at the MP2C and DFT levels.

4. Conclusions

Accurate interaction energy profiles related to the main limiting configurations of the P-CP complex were obtained at the MP2C level of theory. The A1 and A2 parallel approaches provide the most attractive profiles with favourable binding energies (around 500 meV) suggesting that the CP physisorption on G sheets is in principle possible. Interestingly, the minimum for the B1 perpendicular configuration is close in energy but displaced at larger intermolecular distances. This behaviour suggests that, even if the various interaction contributions are likely different for the parallel and perpendicular approaches, their combined effect leads to similar total interaction energies.

The reference MP2C results also served to test and validate several functionals within the DFT ansatz: the PBE(D3)-BJ method was that providing the best agreement together with an affordable computational and it is recommended for the description of the non-covalent interactions in G-CP complexes.

4. References

1. T. C. Johnstone, K. Suntharalingam, S. J. Lippard, *Chem. Rev.* 2016, **116**, 3436–3486.
2. K. Thanli, R.P.Gangwal, A.T.Sangamwar, S.Jain, *Journal of Controlled Release*, 2013,**170**, 15-40.
3. Y. Zhang, H. F. Chan. Kam, W. Leong, *Advanced Drug Delivery Reviews*, 2013, **65**, 104-120.
4. A.K. Geim and K.S. Novoselov, *Nature Materials*, 2007, **6**, 183-191.

5. V. Georgakilas, M. Otyepka, A. B. Bourlinos, V. Chandra, N. Kin, K. C. Kemp, P. Hobza, R. Zboril and K. S. Kim, *Chem. Rev.*, 2012, **6**, 6156-6214.
6. J. Liu, L. Cui, D. Losic, *Acta Biomaterialia*, 2013, **9**, 9243-9257.
7. C. McCallion, J. Burthem, K. Rees-Unwin, A. Golovanov, A. Pluen, *European Journal of Pharmaceutics and Biopharmaceutics*, 2016, **104**, 235-250.
8. S. Syama, P.V. Mohanan, *International Journal of Biological Macromolecules*, 2016, **86**, 546-555.
9. L. A. D. Souza, C. A. S. Nogueira, P. F. R. Ortega, J. F. Lopes, H. D. Calado, R. L. Lavall, G. G. Silva, H. F. D. Santos, and W. B. D. Almeida, *Inorg. Chim. Acta*, 2016, **447**, 38.
10. L. A. D. Souza, C. A. S. Nogueira, J. F. Lopes, H. F. D. Santos, and W. B. D. Almeida, *J. Inorg. Biochem.*, 2013, **129**, 71-83.
11. H. Vovusha, S. Sanyal, B. Sanyal, *J. Phys. Chem. Lett.*, 2013, **4**, 3710-3718.
12. A. Hesselman, T. Korona, *Phys. Chem. Chem. Phys.*, 2011, **13**, 732-743.
13. D. Figgen, K. A. Peterson, M. Dolg, and H. Stoll, *J. Chem. Phys.*, 2009, **130**, 164108.
14. R. A. Kendall, T. H. Dunning, and R. J. Harrison, *J. Chem. Phys.*, 1992, **96**, 6796.
15. J. Perdew, K. Burke, and M. Ernzerhof, *Phys. Rev. Lett.*, 1996, **77**, 3865.
16. P. J. Stephens, F. J. Devlin, C. F. Chabalowski, and M. J. Frisch, *J. Phys. Chem.*, 1994, **98**, 11623.
17. Y. Zhao, D. G. Truhlar, *Theor. Chem. Account.*, 2008, **120**, 215-241.

18. J. S. Binkley, J. A. Pople, and W. J. Hehre, *J. Am. Chem. Soc.*, 1980, **102**, 939.
19. D. Andrae, U. Haeussermann, M. Dolg, H. Stoll, and H. Preuss, *Theor. Chim. Acta*, 1990,**77**, 123.
20. S. Boys and F. Bernardi, *Mol. Phys.*, 1970, **19**, 553.
21. H. B. Jansen and P. Ros, *Chem. Phys. Lett.*, 1969, **3**,140.
22. S. Grimme, S. Ehrlich, and L. Goerigk, *J. Comput. Chem.*, 2011, **32**, 1456.
23. Johnson, E. R.; Becke, A. D. *J. Chem. Phys.*, 2006, **124**, 174104.